PAPER

Enhancing InGaN LED performance via ALD-grown Al_2O_3 sidewall passivation

To cite this article: H M Bayramlı *et al* 2025 *Phys. Scr.* **100** 045902

Physica Scripta

RECEIVED
29 October 2024

REVISED
5 January 2025

ACCEPTED FOR PUBLICATION
13 February 2025

PUBLISHED
6 March 2025

PAPER

Enhancing InGaN LED performance via ALD-grown Al_2O_3 sidewall passivation

H M Bayramlı[1,2], M Genc[3], O Yücel[4], B Bulut[2], A Bek[5,6] and M Demirtas[7,8]

[1] Department of Optics and Photonics Engineering, Bursa Uludağ University, 16059 Bursa, Türkiye
[2] Optoelectronic R&D Center, Ermaksan, Bursa, 16065, Türkiye
[3] Tyndall National Institute, University College Cork, Photonics Group, Cork, T12 R5CP, Ireland
[4] Department of Physics, Freie Universitat Berlin, Arnimallee 14, 14195 Berlin, Germany
[5] Department of Physics, Middle East Technical University, 06800 Ankara, Türkiye
[6] Micro and Nanotechnology Program, Middle East Technical University, 06800 Ankara, Türkiye
[7] Department of Electrical and Electronics Engineering, Bursa Uludağ University, 16059 Bursa, Türkiye
[8] ASELSAN A.S. MEOS Business Sector, P.K. 20, Akyurt 06750, Ankara, Türkiye

E-mail: mustafademirtas@uludag.edu.tr

Keywords: InGaN LEDs, passivation, aluminium oxide, silicon dioxide, long-term stability

Supplementary material for this article is available online

Abstract

InGaN-based light-emitting diodes (LEDs) are at the forefront of solid-state lighting technologies due to their superior efficiency and broad spectral emission. However, their performance is often compromised by leakage currents, which lead to reduced external quantum efficiency. Passivation of surface defect, the need of which arises from either epitaxial growth or mesa etching, emerges as a promising strategy to mitigate leakage currents and enhance LED performance. This study compares the effects of different sidewall passivation using two dielectric materials, Al_2O_3 and SiO_2, on the reliability and long-term stability performance of InGaN LEDs. The study conducts a comprehensive analysis to evaluate the impact of each material on reducing leakage current and improving overall device efficiency. The experimental findings of our study indicate that the LEDs with Al_2O_3 sidewall passivation have better long-term stability performance, lower series resistance, higher breakdown voltages, significantly lower leakage current, and up to a 19% increase in light output power compared to SiO_2 sidewall passivation. These superior properties of Al_2O_3-passivated LEDs increase device reliability and stability. Conversely, SiO_2-passivated LEDs demonstrate relatively higher leakage currents, which can be attributed to lower dielectric constant, non-uniform film deposition and incomplete defect passivation.

1. Introduction

Light-emitting diodes (LEDs) based on Indium Gallium Nitride (InGaN) have emerged as indispensable components in a wide range of optoelectronic applications such as solid-state lighting, displays, optical communications and sensors (Nakamura and Fasol 1997, Pimputkar *et al* 2009). Their exceptional performance, characterized by high efficiency, outstanding brightness, and remarkable reliability, has positioned them at the forefront of technological advancements in these fields (Ji and Liu 2006). Despite their remarkable achievements, InGaN-based LEDs still face a significant challenge that hinders their optimal performance: leakage currents. The emergence of these undesired currents, often originating from intrinsic defects present in the epitaxial layers or surface imperfections introduced during subsequent fabrication processes, can significantly compromise the external quantum efficiency of the LEDs (Miikkulainen *et al* 2002, Lin *et al* 2013). Leakage currents essentially represent non-radiative recombination pathways, diverting essential charge carriers away from the intended light-emitting processes and ultimately diminishing the overall efficiency of the device. This phenomenon translates directly to reduced performance, limiting the full potential of InGaN-based LEDs in practical applications, and hindering further technological advancements.

To overcome the detrimental effects of leakage currents and unlock the full potential of InGaN-based LEDs, researchers have investigated various passivation techniques (Chang *et al* 2001, Adivarahan *et al* 2000, Kim *et al* 2002, Yang *et al* 2012, Liu *et al* 2014, Wong *et al* 2018, Sheremet *et al* 2018). Passivation both electrically and chemically repairs the LED surface and sidewalls created after etching processes during microfabrication. It aims to neutralize active surface states and minimize defect densities by forming a protective layer. This layer effectively suppresses current leakage, leading to enhanced device performance and improved reliability (Elam *et al* 2003, Nakamura and Fasol 1997, Zhang and Zhou 2014). Among the various passivation approaches, Atomic Layer Deposition (ALD) and Plasma-Enhanced Chemical Vapor Deposition (PECVD) have emerged as promising contenders due to their ability to deposit conformal and high-quality thin films with precise control over thickness and composition (Demirtaş *et al* 2018, Demirtaş *et al* 2020).

ALD offers distinct advantages over other passivation methods, particularly in terms of precise control over film thickness and composition and its ability to achieve conformal coverage even on complex geometries. This is achieved through the sequential deposition of atomic layers, ensuring uniform coverage of the LED surface, including sidewalls and high-aspect-ratio structures (Lin *et al* 2013). This unique characteristic makes ALD particularly well-suited for addressing the challenges associated with leakage currents in InGaN-based LEDs, as it can effectively passivate surface defects and minimize current leakage pathways.

Previous research has explored various passivation techniques to mitigate leakage currents in InGaN-based LEDs. Investigations by Lin *et al* (2013) explored alternative approaches to address leakage currents and enhance the performance of InGaN-based LEDs . However, further optimization is still needed to unlock the full potential of these devices and drive technological advancements in various fields. Wong *et al* (2019) reported that the combination of ALD-coated SiO_2 and KOH chemical treatment improved the ideality factor and external quantum efficiency (EQE) of micro-LEDs. A hybrid QD-NR-μLED with an ALD passivation layer and efficient non-radiative energy transfer (NRET) demonstrated a 143.7% increase in light-emitting intensity, reduced exciton recombination lifetime, improved NRET efficiency (66.4% versus 53.6%), and excellent color performance (Chen *et al* 2019). In 2020, Ley *et al* (2020) employed chemical etching and Al_2O_3 dielectric passivation to mitigate sidewall defects, leading to improved EQE. The use of ALD sidewall passivation in AlGaInP micro-LEDs was also shown to enhance electrical and optical performance by reducing leakage, boosting light output, and increasing EQE by over 150%, making them ideal for red emitters in full-color μLED displays (Wong *et al* 2020). Lai *et al* (2022) demonstrated that ALD sidewall passivation significantly improved the temperature stability, light extraction efficiency, and current density distribution of mini-LEDs, thereby enhancing their overall performance and reliability. Moreover, Wong *et al* (2024) showed that a novel deep-ridge laser structure with ALD sidewall passivation improved optical characteristics, reduced internal loss, and enhanced the optoelectrical performance and lifespan of 8 μm ridge width III-nitride violet lasers on freestanding m-plane GaN substrates.

This study investigates the impact of sidewall passivation using two dielectric materials, Al_2O_3 and SiO_2, on the reliability and long-term stability performance of InGaN LEDs. A thorough analysis was performed to assess how each material influences leakage current reduction and overall device efficiency. The experimental results show that LEDs with Al_2O_3 sidewall passivation exhibit superior and long-term stability performance, reduced series resistance, higher breakdown voltages, significantly lower leakage current, and up to a 19% increase in light output power compared to those with SiO_2 passivation. These enhanced characteristics of Al_2O_3-passivated LEDs contribute to greater device reliability and stability. In contrast, SiO_2-passivated LEDs exhibit higher leakage currents, likely due to a lower dielectric constant, non-uniform film deposition, and incomplete defect passivation.

2. Materials and methods

The epitaxial structure and fabrication steps of LED is illustrated in figure 1. InGaN-based LED samples were prepared using metalorganic chemical vapor deposition (MOCVD) on c-plane sapphire substrates. The epitaxial structure consisted of a 3 μm thick undoped GaN buffer layer, a 2 μm thick n-type GaN layer, multiple InGaN/GaN quantum wells (QWs) with varying indium composition and a 200 nm thick p-type GaN layer. The growth temperature was maintained at 1050 °C, and the flow rates of trimethylgallium (TMGa), trimethylindium (TMIn), and ammonia (NH_3) were adjusted to achieve the desired indium content and QW thickness. The structure consists of 15 pairs of InGaN/GaN quantum wells, with each pair consisting of a 3 nm InGaN well and a 13 nm GaN barrier layer. The indium content in the well is 15% ($In_{0.15}Ga_{0.85}N$).

The LED structures grown using metalorganic chemical vapor deposition (MOCVD) were employed. Commercial LED structures are typically grown on sapphire substrates. In addition to light emission, ensuring the efficient extraction of light is essential due to differences in refractive indices. One fundamental method for achieving this is epitaxial growth on patterned sapphire substrates, facilitating the scattering of light produced in

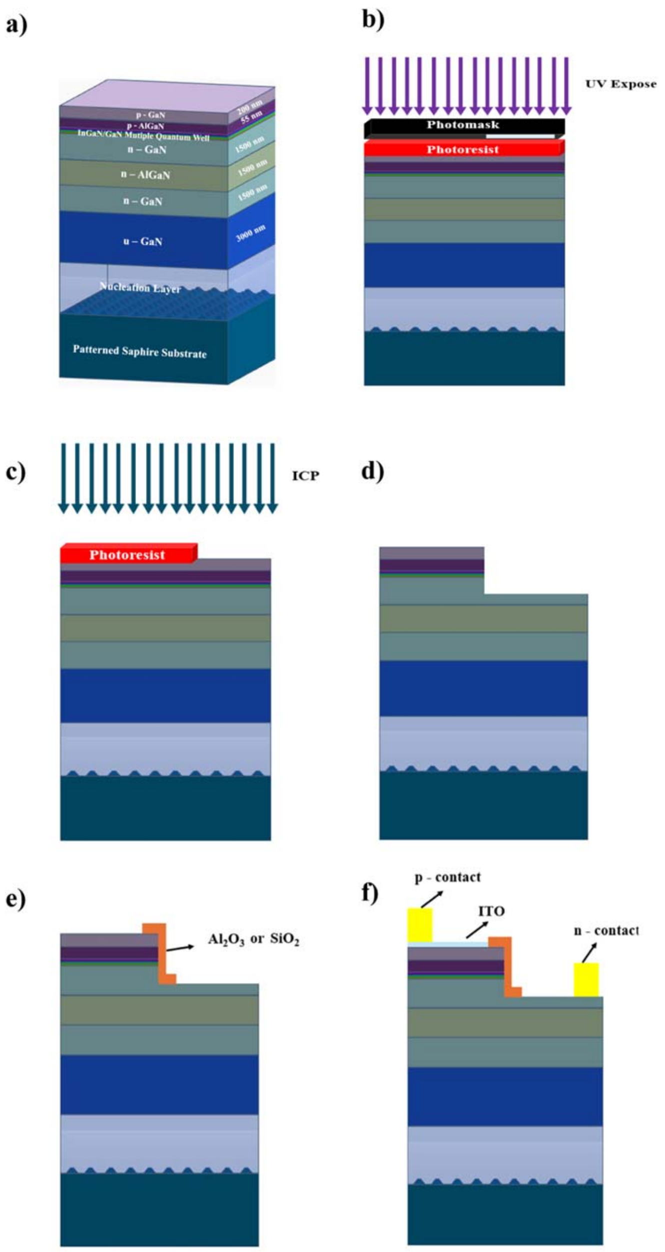

Figure 1. Fabrication steps. (a) The epitaxial structure of the fabricated LEDs. (b) lithography stage (c) ICP etching (d) sample etched down to the n-GaN layer (e) sidewall passivation (Al_2O_3 and SiO_2) (f) coating of contact metals.

the active region. LEDs grown on patterned sapphire substrates exhibit lower total internal reflection compared to those grown on flat sapphire substrates, resulting in higher optical efficiency (Zhou *et al* 2015).

Another advantage of LED layer grown on patterned sapphire substrates is the lower defect density compared to LEDs grown on flat sapphire substrates due to the mismatch in lattice constants between sapphire and GaN crystals. These defects, affecting electrical and optical properties such as electron mobility and radiative recombination efficiency, shorten device lifetimes. Lower defect density leads to higher light output power. Figure 2 presents optical microscope images illustrating the passivation films both before and after LED fabrication, including the passivation film etch process.

The device dimensions are 850 μm $\times$ 850 μm. The p-contact area is formed by coating the topmost p-GaN layer with ITO, excluding the etched regions. The n-contact area is approximately 250 μm $\times$ 250 μm.

Two dielectric materials were employed in this study: aluminum oxide (Al_2O_3) and Silicon Dioxide (SiO_2). For Al_2O_3 passivation, Beneq TFS200 ALD system was used. Trimethylaluminum (TMA) and water vapor (H_2O) were used as precursors, with a deposition temperature of 250 °C and a pulse/purge sequence of 0.1 s/3 s. Ultrahigh pure N_2 gas is continuously used as both the carrier and purge gas during the precursor delivery and pumping processes. Throughout the deposition process, the N_2 flow rate is maintained at 300 sccm. After the coatings were applied, a 75 °C solution of 85% phosphoric acid (H_3PO_4) was used to remove Al_2O_3 films

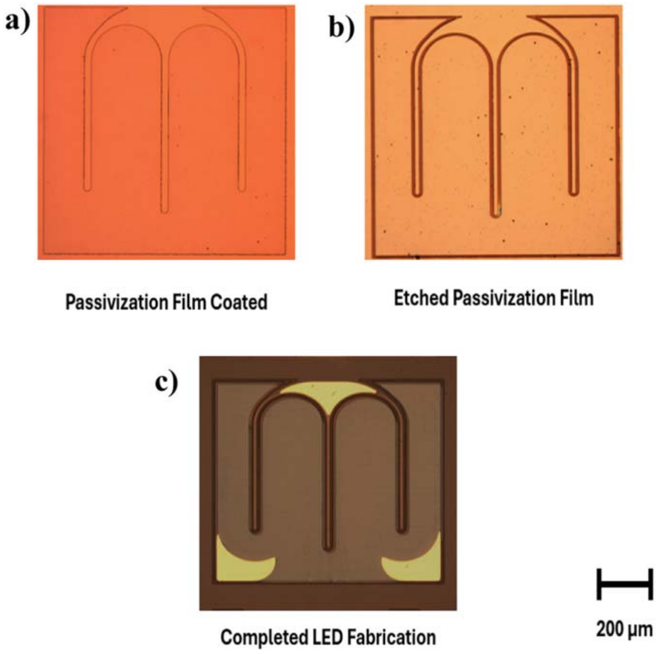

Figure 2. Optical microscope images showing the (a) passivation films before LED fabrication, (b) after passivation film etching, and (c) upon completion of LED fabrication.

deposited by ALD from the regions outside the sidewalls. The H_3PO_4 solution was heated on a hot plate at 75 °C. Subsequently, the samples were immersed in the H_3PO_4 solution and kept submerged. After approximately 90 s, the samples were removed from the phosphoric acid, rinsed with deionized (DI) water, and dried with nitrogen gas. The etching rate in this recipe was approximately 40–45 nm min^{-1}.

The SiO_2 films grown by Plasma-Therm PECVD were produced at 250 °C using a gas mixture of 50 sccm 2% SiH_4/N_2 and 1000 sccm N_2O. The SiO_2 layers etched in buffered oxide etchant (BOE) for approximately 80 s. The passivation films on the sidewalls were protected by photolithography using a photoresist. The growth recipe and etching procedure can be found in (Ay and Aydinli 2004, Demirtaş *et al* 2018, Demirtaş *et al* 2020, Demirtaş and Ay 2020).

Figure 3 illustrates Spectroscopic Ellipsometer (SE), and x-ray reflectance (XRR) measurements conducted on dielectric materials deposited onto a Si substrate. The XRR measurements were performed using the Rigaku Smartlab XRD system, while spectroscopic ellipsometry measurements were conducted with the J.A. Woolam M2000 instrument. The SE measurements aimed to determine the refractive index, thickness, and surface roughness of the deposited films. The SE data were analyzed at various angles (60°, 65°, 70°, and 75°), and mean square error (MSE) values were calculated from the measurements to evaluate the fit quality between the experimental and modeled data, thereby assessing the roughness and thickness of the samples. The Cauchy and Sellmeier equations are employed as fitting functions for Al_2O_3 and SiO_2, respectively (Al-Ani 2008, Tan 1998). The results revealed that the Al_2O_3 films exhibited lower both MSE and roughness compared to the SiO_2 films, indicating a better agreement between the measured and modeled data.

XRR measurements, performed via the reflection of x-ray beams at grazing incidence above a critical angle, serve to determine crucial parameters such as thickness, density, and interfacial roughness, essential for this investigation. The blue curves represent the measured data, while the red curves depict calculated values based on these measurements, with accompanying fit results presented in a table within the XRR graphs. In the fitting process, three additional layers were considered besides the substrate: 'Layer1' accounts for the material interface between the substrate and the coated dielectric, incorporating factors such as substrate impurities, residual atoms, and lattice mismatch effects. 'Layer2' represents the coated dielectric material, while 'Layer3' addresses potential surface contamination from residual atoms in the reactor chamber and impurities from the external environment. Comparison of interface roughness between SiO_2 films and Al_2O_3 films deposited on Si reveals that the Al_2O_3 films exhibit abrupt interfaces. The distinctive density observed in 'Layer1' suggests the formation of a thin SiO_x layer between the Si substrate and Al_2O_3, potentially arising from oxygen diffusion through the deposited Al_2O_3 film or reaction of Si surface groups with H_2O during Al_2O_3 deposition (Renault *et al* 2002, Naumann *et al* 2012a, 2012b, Gakis *et al* 2019). These findings highlight the superior suitability of Al_2O_3 for sidewall passivation, attributed to its smoother atomic interface and higher density compared to SiO_2.

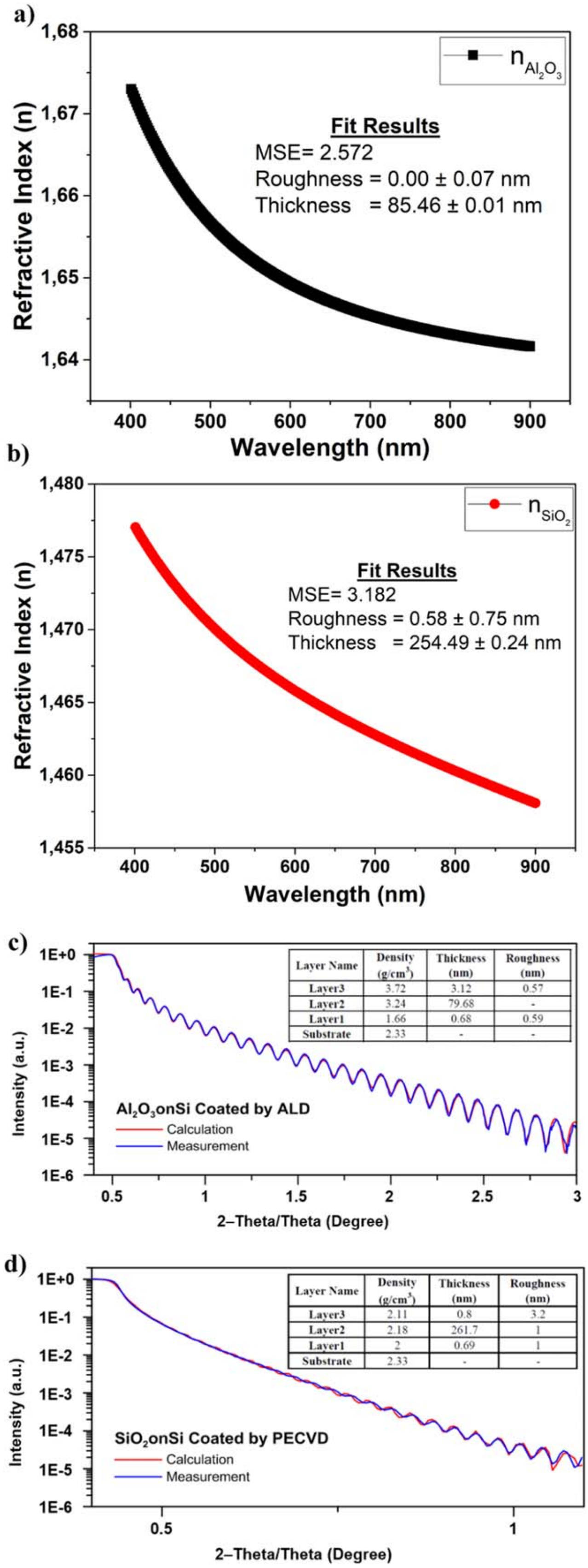

Figure 3. Optical characterization of passivation layers. The SE measurements depicting refractive index versus wavelength for (a) Al_2O_3 and (b) SiO_2 layers, alongside the XRR measurements illustrating (c) Al_2O_3 and (d) SiO_2.

The XRR and SE measurements have provided consistent results for the thickness and roughness of the thin films analyzed. The thickness values obtained from both the XRR and SE techniques exhibited close agreement, indicating the reliability and accuracy of the measurements across different experimental methods.

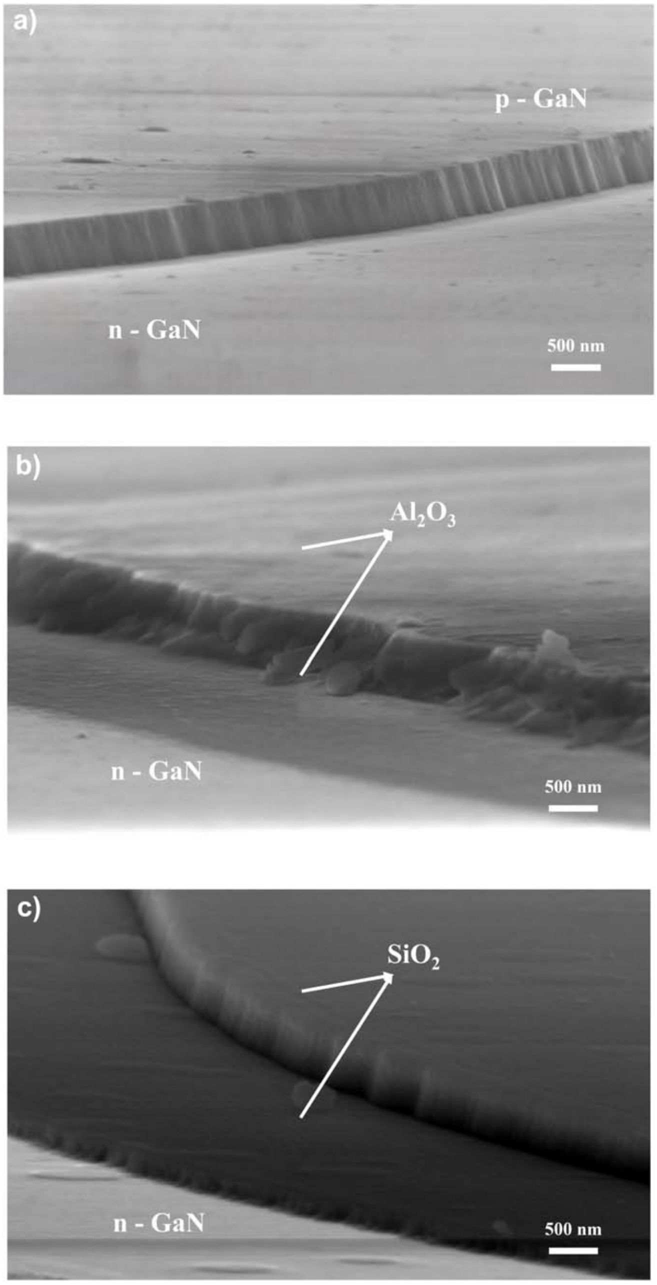

Figure 4. Cross-sectional scanning electron microscopy (SEM) images illustrating sidewall profiles of fabricated LEDs. (a) Sidewall without passivation film coating, with passivation coatings of (b) Al_2O_3, and (c) SiO_2.

Additionally, the roughness parameters determined through the XRR analysis were found to be consistent with the roughness values obtained from the SE, further corroborating the coherence and reliability of the data.

Figure 4 illustrates cross-sectional scanning electron microscopy (SEM) images depicting the sidewall profiles of the fabricated LEDs. In figure 4(a), the sidewall is depicted without any passivation film coating. Subsequently, figure 4(b) displays Al_2O_3 passivation films coated on the sidewalls, while figure 4(c) showcases LEDs with SiO_2 coating on the sidewalls. Scanning electron images were obtained with an acceleration voltage of 18 kV and a magnification of 50 kX using the FEI Nova NanoSEM 450.

Following the passivation step, the n-type contact layer of the samples was coated with Ti/Al/Ti/Au. The p-type contact layer was coated with Ni/Au/ITO acts both as an ohmic contact and current-spreading layer. Rapid Thermal Annealing (RTA) was applied to the contacts to ensure ohmic behavior. The thickness of the deposited films was measured using a Veeco surface profilometer.

Current–voltage (I-V) measurements were performed using a semiconductor parameter analyzer (Keithley 2425) to assess the leakage currents of the passivated LEDs. The optical properties of the devices were evaluated using a calibrated spectroradiometer (Ocean Optics Maya2000 Pro) to measure the electroluminescence spectra and output power. To prevent accidental overcurrent before measurements, current limiting is applied and then

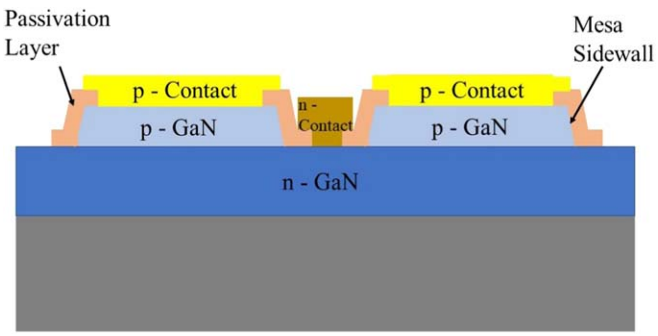

Figure 5. The schematic view of the fabricated LEDs with side walls and contacts.

the current is increased at a controlled rate using a computer. The current and voltage values are recorded simultaneously. Due to the small size of the LED chips, the probe tips are gently touched to the n-type and p-type contacts with the aid of a microscope. Using this method, several LEDs with various geometries were measured to create current–voltage curves. The curves provide valuable insights into the electrical characteristics of the LEDs, such as their turn-on voltage, forward current, and reverse breakdown voltage. These parameters are essential for designing and optimizing LED circuits and predicting LED performance in different applications.

The surface morphology of the passivated LED samples was examined using atomic force microscopy (AFM). The AFM measurements were conducted with a Nanomagnetics ezAFM system in tapping mode.

Average roughness (Ra) measurements were conducted using AFM on 20 μm × 20 μm areas deposited on Si substrate. The roughness of the Si substrates was ∼0.58 nm. For Al_2O_3 films ranging from 5 to 100 nm in thickness, the average roughness is ∼0.71 nm based on four measurements and remained stable as the thickness increased. Additionally, PECVD grown SiO_2 layer deposited on Si substrate has an average roughness of 2.61 nm (the results provided in the supplementary document).

3. Results

It was previously noted that p-type doping of GaN crystals with Mg does not increase the conductivity of p-GaN layers, even with doping levels exceeding 5×10^{17} Mg cm^{-3} (Amano *et al* 1989, Nakamura *et al* 1992, Li *et al* 2016). Therefore, contacts to the p-GaN layer were placed at the top and designed to cover the widest possible area to reduce series resistance. The doping concentrations used in the study are as follows: n-GaN = 3×10^{18} cm^{-3} and p-GaN = 4×10^{17} cm^{-3}. Inductively coupled plasma (ICP) reactive ion etching was employed to etch down to the n-GaN layer at the other end of the diode. This process allowed access to the n-GaN layer, with a portion etched in a thin finger geometry. After applying the passivation layer, windows were opened in the passivation film on the metal n-GaN layer, and n-type contacts were applied. Despite the small size of the n-contact area, the high doping level of the n-GaN layer makes it a good conductor, leading to current spreading in this layer and consequently increasing optical efficiency and reducing series resistance. Figure 5 provides a side view of the produced LEDs, where increasing the number of n-contacts reduces the p-contact area and tends to increase series resistance.

As depicted in figure 6, it can be observed that SiO_2-passivated LED exhibits higher current density at low voltage values and higher leakage current compared to Al_2O_3-passivated LED. Therefore, it can be inferred that the threshold voltage (approximately 1.7 V for the SiO_2-passivated LEDs) is lower. The excess current values observed at low voltages near the threshold current under forward bias are related to leakage currents, while the high voltage values are associated with series resistance. The leakage current caused by sidewall defects, defects in the active region, and low barrier height results in a lower threshold voltage in diodes (Li *et al* 2004, Schubert 2006).

Figure 7 illustrates that the typical series resistance for the Al_2O_3-passivated LED is 11.8 Ω, while for the SiO_2-passivated LED, it is 12.5 Ω. The high series resistance is due to the fact that the LEDs are not flip chips and the masks are designed to compare the two passivation techniques more effectively. It was found that the Al_2O_3-passivated LEDs exhibited lower series resistance compared to the SiO_2-passivated LEDs, indicating better electrical performance. The series resistance can be attributed to factors such as high contact resistance, surface damage, surface cleanliness, lattice constant mismatched heterostructures, layers with low carrier concentration, and temperature effects (Cao *et al* 2004). The higher series resistance in the SiO_2-passivated LEDs can be explained by the increase in non-radiative recombination, which elevates the device temperature

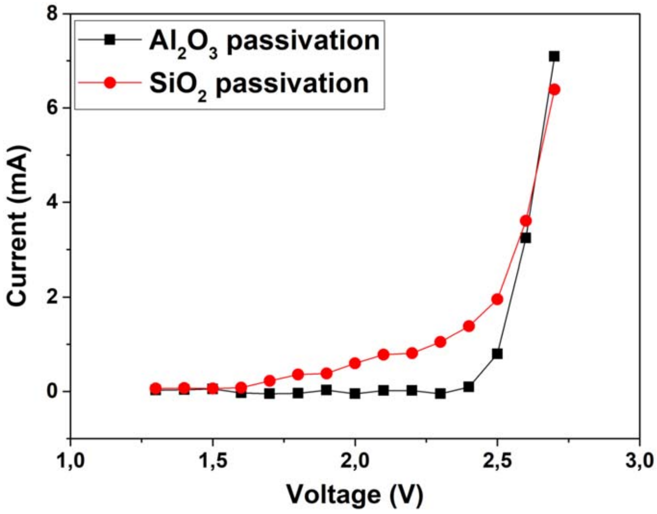

Figure 6. The current–voltage (I-V) characteristics around the threshold voltage of the Al_2O_3-passivated and SiO_2-passivated LEDs.

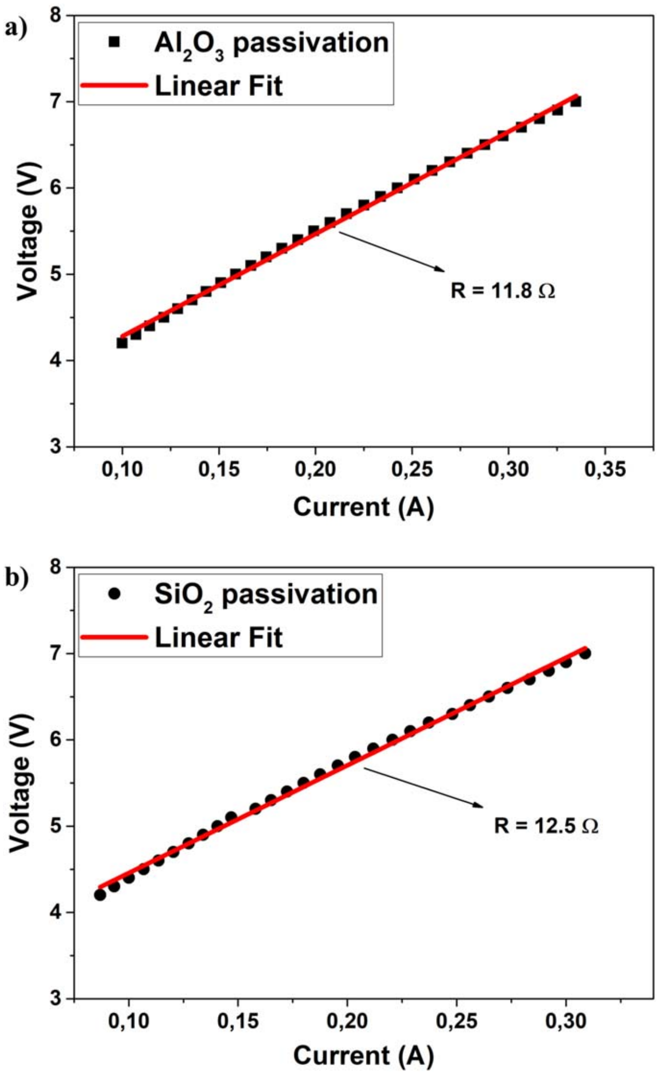

Figure 7. Measurement of the series resistance of fabricated LEDs passivated with (a) Al_2O_3 and (b) SiO_2.

(Schubert 2006). Another contributing factor to the increased series resistance in the SiO_2-passivated LEDs may be the re-exposure to plasma during the passivation film deposition, leading to the passivation of p-GaN layer by hydrogen atoms, thereby increasing the resistance of the p-GaN layer.

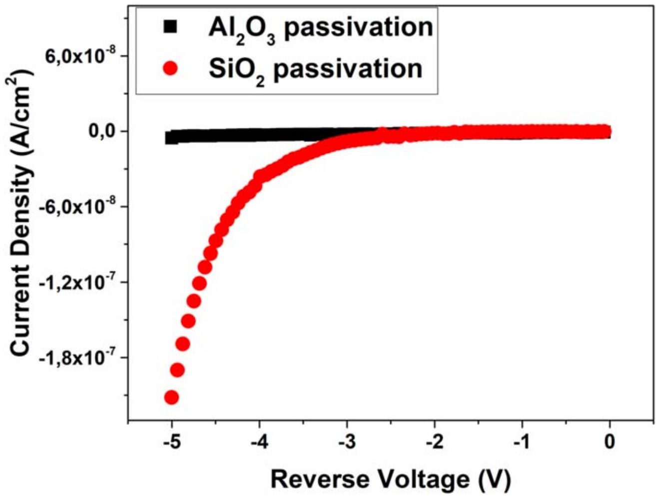

Figure 8. Typical reverse voltage-current density graph of both Al_2O_3 and SiO_2-passivated LEDs.

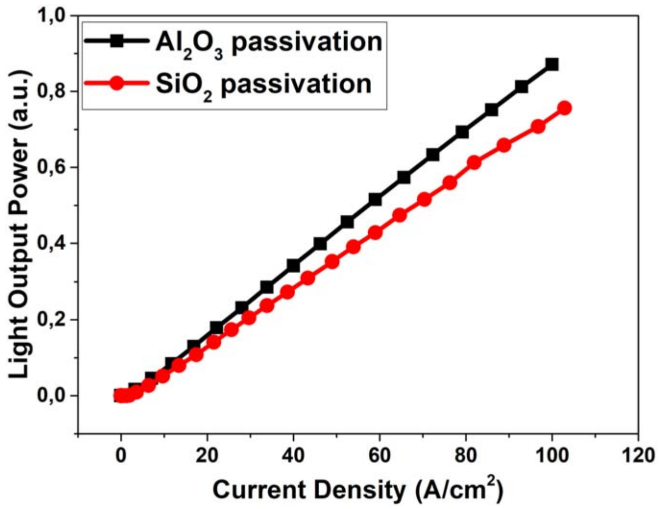

Figure 9. The I-P (current and optical power) graph of the Al_2O_3-passivated and SiO_2-passivated LEDs.

The Al_2O_3 and SiO_2-passivated LEDs are investigated for their leakage current effects under reverse bias voltages ranging from −5 V to 0 V. Figure 8 illustrates the current density under reverse bias of both Al_2O_3 and SiO_2-passivated LEDs. Notably, the Al_2O_3-passivated LED exhibits an extremely low leakage current density, approximately 10^{-9} A/cm^2. These findings underscore the significant role of Al_2O_3 passivation in mitigating leakage current and preventing sidewall damages across all structures.

The optical power measurements of both Al_2O_3 and SiO_2-passivated LEDs were conducted using a Newport Power Meter Model 1936-C power meter. The optical power measurement involved collecting light emitted from the produced LEDs using a lens with a diameter of 25 mm and a focal length of 5 cm, which was then directed toward the detector of the power meter. Figure 9 presents the current density (I) - optical power (P) graphs for Al_2O_3 and SiO_2-passivated LEDs. It is observed that the optical power of the Al_2O_3-passivated LEDs is superior to that of SiO_2-passivated LEDs. This phenomenon can be attributed to higher dielectric constant and the better passivation of sidewall surface defects and the near-sidewall non-radiative recombination centers by ALD, thereby increasing the probability of radiative recombination. As a result, the Al_2O_3-passivated LEDs exhibit reduced non-radiative recombination centers near the sidewalls and prevent the temperature increase resulting from non-radiative recombination, leading to higher light power compared to the SiO_2-passivated LEDs.

The External Quantum Efficiency (EQE) and Wall Plug Efficiency (WPE) are also evaluated as functions of the driven current. The LEDs passivated with Al_2O_3 exhibit superior EQE and WPE compared to those passivated with SiO_2 (the results provided in the supplementary document). These findings suggest that Al_2O_3 more effectively passivates sidewall defects. Particularly at lower current levels, the EQE values are influenced by

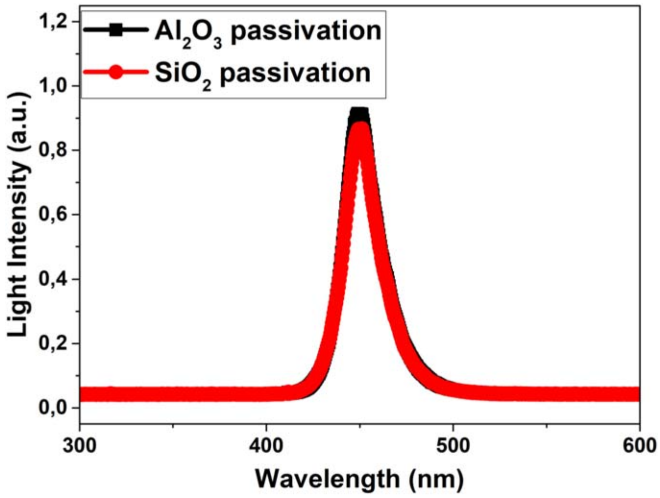

Figure 10. The emission spectra of both Al_2O_3 and SiO_2-passivated LEDs. Both emissions are at 450 nm.

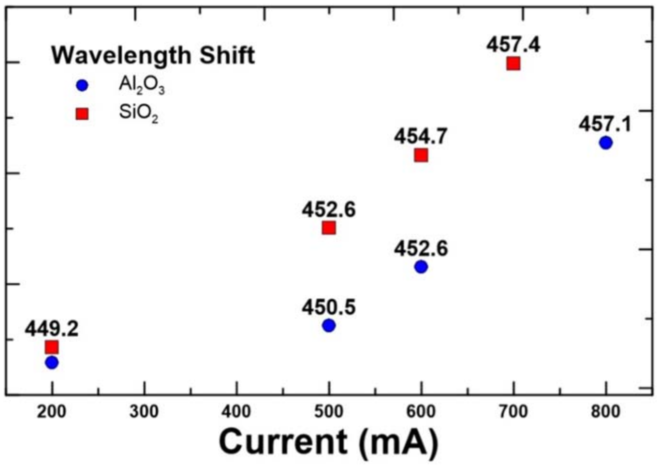

Figure 11. The wavelength variation of light emitted as a function of current from Al_2O_3 and SiO_2 passivated LEDs stored 4-years under normal conditions.

defects and non-radiative recombination processes. Additionally, the enhanced performance can be attributed to the superior step coverage capability of the Atomic Layer Deposition (ALD) technique.

The Electroluminescence (EL) measurements of the LEDs were conducted using the Ocean Optics Maya2000 Pro spectrometer. Figure 10 presents the emission spectra of Al_2O_3 and SiO_2-passivated LEDs. The light intensity of Al_2O_3-passivated LED is higher than that of SiO_2-passivated LED. Additionally, both LEDs exhibit peak wavelengths at 450 nm, indicating no significant impact of passivation on the wavelength. The lower light intensity in the SiO_2-passivated LEDs, which is less effectively passivated at the sidewalls compared to the Al_2O_3-passivated LED, can be attributed to the higher density of defects in the sidewalls of SiO_2-passivated LEDs, resulting in higher non-radiative recombination.

To evaluate reliability and long-term stability performance, LEDs stored under normal conditions for 4 years were used. Using these LEDs, analyses were conducted by investigating the wavelength variation of light emitted from the device, IV measurements, and optical power measurements.

Figure 11 shows the wavelength variation of light emitted from the device with increasing current. For both devices, the epitaxial structure, device design, and microfabrication process are identical. Therefore, the wavelength shift can be attributed to sidewall defects. The increase in defect density on the sidewalls and the higher likelihood of non-radiative recombination lead to a greater wavelength shift with increasing current in LEDs passivated with SiO_2 due to heating. This serves as an indicator of reliability (Keppens *et al* 2010; Raypah *et al* 2016).

Figure 12(a) graph shows the IV characteristics measured after the initial (fresh) microfabrication of the devices and after 4-years. In this graph, an increase in voltage is observed for both devices. However, the

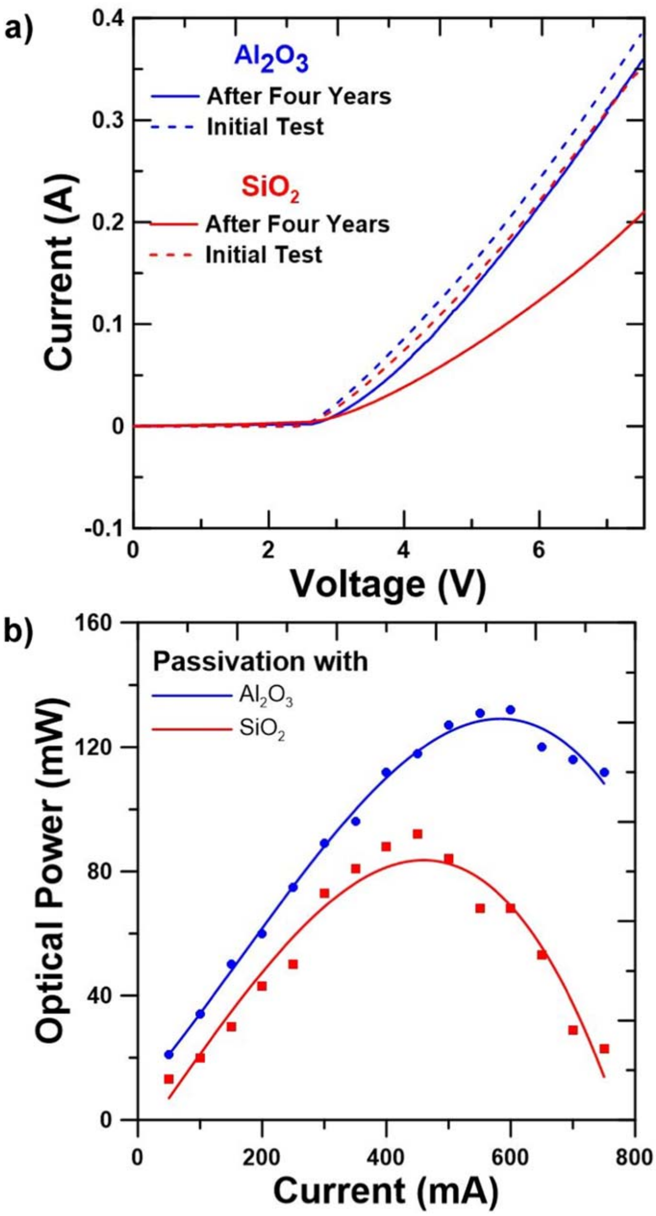

Figure 12. (a) Comparison of I–V curves at the initial stage (fresh) and after a 4-years. Dashed and solid lines show fresh and 4-years old LEDs. (b) Optical power versus current for 4-years old LEDs.

degradation in LEDs with SiO_2 passivation is significantly higher than Al_2O_3 passivation. Therefore, it has been observed that sidewall passivation performed with ALD and Al_2O_3 improves device reliability. Figure 12(b) relates to the power variation of the devices over the years, and a power decline has been observed in both devices. The reduction in power has been particularly significant in devices with SiO_2 passivation. Moreover, while SiO_2-passivated LEDs showed degradation at currents exceeding 750 mA, the LEDs passivated with Al_2O_3 continued to operate at current levels above 800 mA.

In addition to the passivation effects, the optical properties of the films, such as refractive index, transmittance, and thickness, significantly influence the photoelectric performance of LED chips. Al_2O_3 films typically exhibit a higher refractive index (around 1.70) compared to SiO_2 (around 1.45), which can enhance light extraction efficiency, especially in thin-film coatings. Moreover, the thickness of the passivation layer plays a critical role in optical performance. Thinner films tend to have higher transmittance, thereby potentially improving light output. They also provide better conformity and more efficient coverage of surface defects, which reduces non-radiative recombination. In our study, the use of thinner Al_2O_3 films resulted in superior passivation effects, which were crucial for enhancing the optical performance of the LED chips. Thus, while the sidewall passivation effect is important for reducing non-radiative recombination, the optical properties of the films also contribute significantly to the overall photoelectric performance of the LED chip.

4. Conclusion

This study comprehensively evaluated the effectiveness of passivation techniques in enhancing InGaN-based LEDs. In terms of electrical performance, Al_2O_3-passivated LEDs exhibited lower series resistance (11.8 Ω) compared to SiO_2-passivated LEDs (12.5 Ω), indicating superior electrical performance. Additionally, SiO_2-passivated LEDs demonstrated higher current density and leakage currents under forward bias, resulting in a lower threshold voltage of around 1.7 V compared to Al_2O_3-passivated LEDs. Under reverse bias conditions, Al_2O_3-passivated LEDs displayed an extremely low leakage current density of approximately 10^{-9} A/cm^2, whereas SiO_2-passivated LEDs exhibited higher leakage currents. Optical power measurements and electroluminescence (EL) measurements both showed that Al_2O_3-passivated LEDs had superior light output and intensity compared to SiO_2-passivated LEDs, while both having peak wavelengths at 450 nm. Our findings reveal that Al_2O_3 films offers superior passivation compared to SiO_2, leading to significantly reduced leakage currents and enhanced device reliability. This advantage can also be from ALD's precise control over film deposition and composition, achieved through its sequential atomic layer-by-layer growth process. By effectively passivating side wall surface defects and minimizing leakage pathways, Al_2O_3 films increase LED performance, resulting in higher external quantum efficiency and improved reliability. Our work reinforces the importance of ongoing research in mitigating leakage currents in InGaN-based LEDs. Future explorations of novel passivation materials and deposition techniques hold promise for further performance and reliability advancements. Overall, this study contributes significantly to the advancement of InGaN-based LED technology by showcasing the potential of ALD deposited Al_2O_3 films for achieving high-performance and reliable optoelectronic devices across diverse applications.

Acknowledgments

The authors sincerely thank Professor Atilla Aydınlı for his valuable support and contributions to this work. We also extend our gratitude to Professor Feridun Ay and Professor Nihan Kosku Perkgöz from the MIDAS Research Group Facility, within the Department of Electrical and Electronics Engineering, Eskisehir Technical University, Türkiye. Additionally, the authors acknowledge the generous funding support for this study from Bursa Uludağ University (Grant # FGA-2024-1745 and Grant # FAY-2024-1777).

Data availability statement

All data that support the findings of this study are included within the article (and any supplementary files).

Funding

This work was supported by Bursa Uludağ University Research under Project Grant Number FGA-2024-1745 and FAY-2024-1777.

Declarations

The authors declare no conflicts of interest.

Contributions

All authors contributed to the conceptualization, methodology, and writing of the manuscript; formal analysis, supervision, review, and editing of this research work.

ORCID iDs

H M Bayramlı https://orcid.org/0000-0001-7999-9328
M Genc https://orcid.org/0000-0003-1887-3582
O Yücel https://orcid.org/0000-0002-7920-2523
A Bek https://orcid.org/0000-0002-0190-7945
M Demirtas https://orcid.org/0000-0001-6832-4341

References

Adivarahan V, Simin G, Yang J W, Lunev A, Khan M A, Pala N, Shur M and Gaska R 2000 SiO_2-passivated lateral-geometry GaN transparent schottky-barrier detectors *Appl. Phys. Lett.* **77** 863–5

Al-Ani Salwan K 2008 Methods of determining the refractive index of thin solid films *Iraqi J. of Appl. Phys.* **4** 17–23

Amano H, Kito M, Hiramatsu K and Akasaki I 1989 P-type conduction in MgDoped GaN treated with low-energy electron beam irradiation (LEEBI) *Jpn. J. Appl. Phys.* **28** L2112–4

Ay F and Aydinli A 2004 Comparative investigation of hydrogen bonding in silicon based PECVD grown dielectrics for optical waveguides *Opt. Mater.* **26** 33–46

Cao X A, Teetsov J A, Shahedipour-Sandvik F and Arthur S D 2004 Microstructural origin of leakage current in GaN/InGaN light-emitting diodes *J. Cryst. Growth* **264** 172–7

Chang K M, Lang C C and Cheng C C 2001 The silicon nitride film formed by ECR-CVD for GaN-based LED passivation *Physica Status Solidi (a)* **188** 175–8

Chen S-W H *et al* 2019 Full-color monolithic hybrid quantum dot nanoring micro light-emitting diodes with improved efficiency using atomic layer deposition and nonradiative resonant energy transfer *Photon. Res.* **7** 416–22

Demirtaş M and Ay F 2020 High-gain Er3+:Al_2O_3 on-chip waveguide amplifiers *IEEE J. Sel. Top. Quantum Electron.* **26** 3200208

Demirtaş M, Odacı C, Perkgöz N K, Sevik C and Ay F 2018 Low loss atomic layer deposited Al_2O_3 waveguides for applications in on-chip optical amplifiers *IEEE J. Sel. Top. Quantum Electron.* **24** 3100508

Demirtaş M, Odacı C, Shehu Y, Perkgöz N K and Ay F 2020 Layer and size distribution control of CVD-grown 2D MoS2 using ALD-deposited MoO_3 structures as the precursor *Mater. Sci. Semicond. Process.* **108** 104880

Elam J W, Routkevitch D, Mardilovich P P and George S M 2003 Conformal coating on ultrahigh-aspect-ratio nanopores of anodic alumina by atomic layer deposition *Chem. Mater.* **15** 3507–17

Gakis G P, Vahlas C, Vergnes H, Dourdain S, Tison Y, Martinez H and Scheid E 2019 Investigation of the initial deposition steps and the interfacial layer of atomic layer deposited (ALD) Al2O3 on Si *Appl. Surf. Sci.* **492** 245–54

Ji X and Liu Z 2006 Origins of leakage currents in InGaN/GaN multiple quantum well light-emitting diodes *Appl. Phys. Lett.* **88** 241912

Keppens A, Ryckaert W R, Deconinck G and Hanselaer P 2010 Modeling high power light-emitting diode spectra and their variation with junction temperature *J. Appl. Phys.* **108**

Kim H M, Huh C and Park S J 2002 Reduction in leakage current of InGaN-based light-emitting diodes by N2O plasma passivation *In Solid State Lighting II* (International Society for Optics and Photonics) 247–54

Lai S *et al* 2022 The impacts of sidewall passivation via atomic layer deposition on GaN-based flip-chip blue mini-LEDs *J. Phys. D: Appl. Phys.* **55** 374001

Ley R T, Smith J M, Wong M S, Margalith T, Nakamura S, DenBaars S P and Gordon M J 2020 Revealing the importance of light extraction efficiency in InGaN/GaN microLEDs via chemical treatment and dielectric passivation *Appl. Phys. Lett.* **116**

Li D S, Chen H, Yu H B, Jia H Q, Huang Q and Zhou J M 2004 Dependence of leakage current on dislocations in GaN-based light-emitting diodes *J. Appl. Phys.* **96** 1111–4

Li G, Wang W, Yang W, Lin Y, Wang H, Lin Z and Zhou S 2016 GaN-based light-emitting diodes on various substrates: a critical review *Rep. Prog. Phys.* **79** 056501

Lin S Y, Wu C Y, Tsai T M, Chen C W and Kuo H C 2013 Improved output power of GaN-based light-emitting diodes with nano-roughened p-GaN surface derived from SiO2 nanosphere lithography masks *Nanoscale Res. Lett.* **8** 1–6

Liu H Y, Hsu W C, Chou B Y, Wang Y H, Sun W C, Wei S Y and Yu S M 2014 Al_2O_3 passivation layer for InGaN/GaN LED deposited by ultrasonic spray pyrolysis *IEEE Photonics Technol. Lett.* 1243–6

Miikkulainen V, Leskelä M, Ritala M and Puurunen R L 2002 Crystallinity of inorganic films grown by atomic layer deposition: overview and general trends *J. Appl. Phys.* **92** 6212–27

Sheremet V *et al* 2018 Two-step passivation for enhanced InGaN/GaN light emitting diodes with step graded electron injectors *Superlattices Microstruct.* **113** 623–34

Nakamura S and Fasol G 1997 *The blue laser diode: GaN based light emitters and lasers* (Springer Science & Business Media)

Nakamura S, Mukai T, Senoh M and Iwasa N 1992 Thermal annealing effects on ptype Mg-doped GaN films *Jpn. J. Appl. Phys.* **31** L139

Naumann V, Otto M, Wehrspohn R B and Hagendorf C 2012a Chemical and structural study of electrically passivating Al_2O_3/Si interfaces prepared by atomic layer deposition *Journal of Vacuum Science & Technology* A **30** 04D106

Naumann V, Otto M, Wehrspohn R B, Werner M and Hagendorf C 2012b Interface and material characterization of thin ALD-Al_2O_3 layers on crystalline silicon *Energy Procedia* **27** 312–8

Pimputkar S, Speck J S, DenBaars S P and Nakamura S 2009 Prospects for LED lighting *Nat. Photonics* **3** 180–2

Raypah M E, Devarajan M and Sulaiman F 2016 Influence of injection current and ambient temperature on intensity and wavelength of low-power SMD LED *IEEE 37th Int. Electronics Manufacturing Technology (IEMT) & 18th Electronics Materials and Packaging (Emap) Conf.* 1–6

Renault O, Gosset L G, Rouchon D and Ermolieff A 2002 Angle-resolved x-ray photoelectron spectroscopy of ultrathin Al_2O_3 films grown by atomic layer deposition *Journal of Vacuum Science & Technology A: Vacuum, Surfaces, and Films* **20** 1867–76

Schubert E F 2006 *Light Emitting Diodes* (Cambridge University Press)

Tan C Z 1998 Review and analysis of refractive index temperature dependence in amorphous SiO_2 *Journal of Non-Crystalline Solids* **238** 30–6

Wong M S *et al* 2020 Improved performance of AlGaInP red micro-light-emitting diodes with sidewall treatments *Opt. Express* **28** 5787–93

Wong M S *et al* 2024 III-nitride m-plane violet narrow ridge edge-emitting laser diodes with sidewall passivation using atomic layer deposition *Opt. Express* **32** 20483–90

Wong M S, Hwang D, Alhassan A I, Lee C, Ley R, Nakamura S and DenBaars S P 2018 High efficiency of III-nitride micro-light-emitting diodes by sidewall passivation using atomic layer deposition *Opt. Express* 21324–31

Wong M S, Lee C, Myers D J, Hwang D, Kearns J A, Li T and DenBaars S P 2019 Size-independent peak efficiency of III-nitride micro-light-emitting-diodes using chemical treatment and sidewall passivation *Appl. Phys. Express* **12** 097004

Yang C-M, Kim D-S, Lee S-G, Lee J-H, Lee Y and Lee J-H 2012 Improvement in electrical and optical performances of GaN-based LED With SiO_2/Al_2O_3 double dielectric stack layer *IEEE Electron Device Lett.* **564** 566

Zhang Y and Zhou Y 2014 Effects of post-deposition annealing on properties of Al_2O_3 films deposited by thermal and plasma-enhanced atomic layer deposition *Appl. Surf. Sci.* **314** 896–901

Zhou S, Yuan S, Liu Y, Guo L J, Liu S and Ding H 2015 Highly efficient and reliable high power LEDs with patterned sapphire substrate and strip-shaped distributed current blocking layer *Appl. Surf. Sci.* **355** 1013–101